Journal of Applied Polymer Science

Freeze-drying method prepared UHMWPE/CNTs composites with optimized micromorphologies and improved tribological performance

Jie Fang,[1] Liubing Dong,[1,2] Wei Dong,[1] Sum Wai Chiang,[1,3] Simo Makimattila,[3] Hongda Du,[1] Jia Li,[1] Feiyu Kang[1,2]

[1]Key Laboratory of Thermal Management Engineering and Materials, Graduate School at Shenzhen, Tsinghua University, Shenzhen City, Guangdong Province 518055, China

[2]State Key Laboratory of New Ceramics and Fine Processing, School of Materials Science and Engineering, Tsinghua University, Beijing 100084, China

[3]KONE China Co. Ltd., No.88 Middle Gu Cheng Road, Yushan Town, Kunshan, Jiangsu, China

Correspondence to: H. Du (E-mail: duhd@sz.tsinghua.edu.cn)

ABSTRACT: Uniformly dispersed carbon nanotubes (CNTs) reinforced ultrahigh molecular weight polyethylene (UHMWPE) composites were successfully prepared by freeze-drying method. Specifically, polymer powders were mixed with CNT aqueous paste, and then freeze-dried. As a consequence, CNTs covered at the surface of UHMWPE powders evenly when CNT content was not very high, which improved the quantity of crystals and crystallinity of UHMWPE/CNTs composites by providing more nucleation sites during the upcoming compression-molded process. Furthermore, optimized dispersion state of CNTs and concomitant higher crystallinity made freeze-drying technique prepared composites display much lower wear rate when compared with pure UHMWPE and UHMWPE/CNTs composites fabricated by common heat-drying method. In a word, our proposed method of freeze-drying is simple and effective for mass production of UHMWPE/CNTs composites, and it is promising to be applied to fabricate many kinds of nanofillers modified polymer composites, for example, polymer/graphene material. © 2015 Wiley Periodicals, Inc. J. Appl. Polym. Sci. **2015**, *132*, 41885.

KEYWORDS: composites; differential scanning calorimetry; friction; graphene and fullerenes; lubrication; nanotubes; wear

Received 11 September 2014; accepted 14 December 2014
DOI: 10.1002/app.41885

INTRODUCTION

Ultrahigh molecular weight polyethylene (UHMWPE) is a polymer with good mechanical and tribological properties, such as notched impact strength and sliding abrasion resistance.[1] It has been widely used for pickers, bumpers, linings, and sidings in industrial fields.[2] However, it is seen restricted in other demanding tribological applications because of some factors, such as load bearing capacity and thermal instability.[3] Several approaches have been taken to improve the wear properties of UHMWPE through the incorporation of zinc oxide,[4] silicon carbide,[5] and other reinforcing additives.[6,7]

As nanoscale fillers with outstanding mechanical and thermal properties, carbon nanotubes (CNTs) have caught great interests to improve tribological performance of UHMWPE-based material, and some researches were developed to prepare UHMWPE/CNTs composites.[8–13] Dry mixing[8,9] is a simple method, but in the method prepared composites, the nanofillers are easy to aggregate resulting from the Van der Waals force among them.[14] Subsequently, solution method[10,11] and *in situ* polymerization[12,13] were exploited. Although the dispersion status of CNTs could be improved, the dispersion medium (e.g., toluene) often causes environmental issue. Moreover, both methods are high cost and unsuitable for industrialized production partly for the complicated producing process or/and large demand for organic solvent. Therefore, a low-cost and simple method is needed to develop and to fabricate UHMWPE/CNTs composites with uniformly dispersed CNTs.

Recently, freeze-drying technique was used in epoxy based composites.[15,16] It is an effective method to optimize CNT distribution state. Fortunately, this technique has been widely applied in food industry[17] and botanical medicine,[18] indicating its simplicity and environment-friendliness (the dispersion medium is water). In this work, we attempted to utilize such method to prepare UHMWPE/CNTs composites. Characterization of dispersion status of CNTs and evaluation of tribological properties of these corresponding composites were conducted. For comparison, the usually used method of heat-drying was also used to prepare the UHMWPE/CNTs composites.

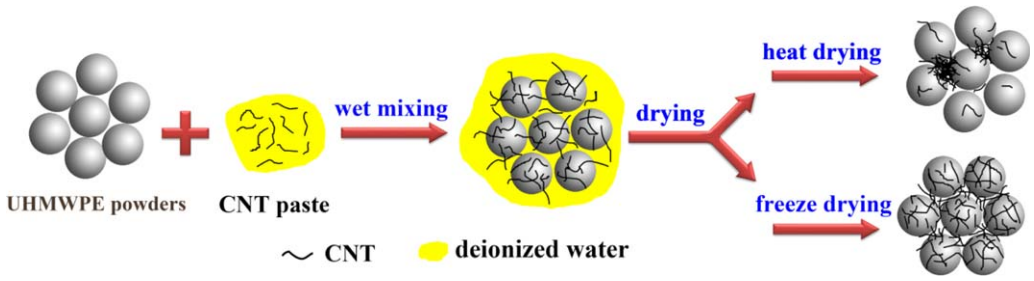

Figure 1. Experiment procedures of preparing UHMWPE/CNTs powders. Effect of different drying methods on CNT dispersion status is shown in the schematic diagram. [Color figure can be viewed in the online issue, which is available at wileyonlinelibrary.com.]

EXPERIMENTAL

Materials

UHMWPE, a granular molding powder obtained from Mitsui Chemicals, Inc., was used in this work. CNT aqueous paste was purchased from Shenzhen Nanotech Port Co. China, and the weight fraction of CNTs was about 5%. These CNTs, with diameter of 15–30 nm and length of 5–15 μm, were synthesized by chemical vapor deposition.

Preparation of UHMWPE/CNTs Composites

Preparation procedures of the UHMWPE/CNTs powders using different drying methods were illustrated in Figure 1. The purchased CNT paste was diluted by deionized water through mechanical mixing and ultrasound. Then it was mixed with UHMWPE powders by a planetary centrifugal mixer (supplied by Shenzhen Hasai Technology Co.) to obtain homogeneous UHMWPE/CNTs slurry. Weight ratio of CNTs : UHMWPE : deionized water was set to be x : 100 : 50, where $x = 0.05$, 0.5, 1, and 2, respectively, in different samples. Then, the slurry was dried by freeze-drying method. In detail, the slurry was quickly frozen by liquid nitrogen, which was beneficial for dispersion of CNTs,[19] and followed by continuous drying in a freezing dryer for ~12 h. As for the commonly used heat-drying method, the well-mixed UHMWPE/CNT slurry was dried by keeping at 50°C for 24 h.

The dried powders were hot-pressed at 180°C with the pressure of 15 MPa for 15 min, and then cooled down to room temperature by water-cooling. The pure UHMWPE sample was compression-molded under the same condition to serve as a baseline.

Characteristics

Features of raw materials and micromorphologies of dried UHMWPE/CNTs powders were observed using scanning electronic microscope (SEM. Model: HITACHI S4800, Japan), with all samples gold coated before testing. Transmission electron microscope (TEM. Model: JOEL JEM-2100F, Japan) was utilized to investigate the microstructure of pristine CNTs. Differential scanning calorimetry (DSC. Model: STA449-F3, Germany) test was performed under nitrogen atmosphere with a temperature range of 30–200°C at a rate of 5°C/min.

Tribological properties of composites were tested using a reciprocating-type ball-on-disc tribometer (HSR-2M, China). The steel ball samples (Model: GCr15 with diameter of 6.35 mm), used as the counterparts, were initially cleaned by sonication in alcohol and dried at 80°C. The surface roughness of balls and disc are below 0.02 μm and 0.05μm, respectively. Tests were conducted at a normal applied load of 20 N with an average sliding speed of 0.2 m/s. The magnitude of contact stress is 18.7 MPa, estimated by using Hertz's elastic contact theory. Each test lasted for 2 h at room temperature without lubrication. Worn surface of these samples were then studied using an optical microscope.

RESULTS AND DISCUSSION

Characteristic of UHMWPE/CNTs Powders

Morphologies of the as-received UHMWPE powders and CNTs were analyzed by SEM and TEM, respectively. Figure 2(a) shows that pure UHMWPE powder is made up of many micronscale

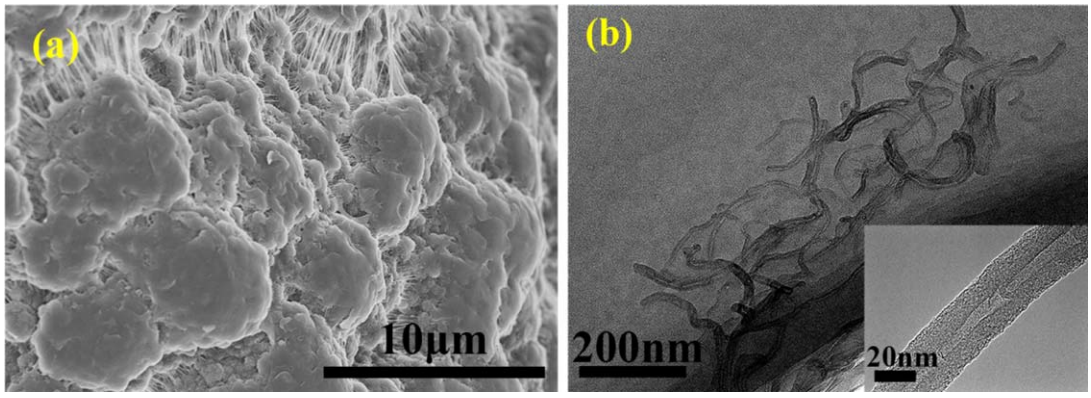

Figure 2. (a) SEM image of UHMWPE powders; (b) TEM images of CNTs. [Color figure can be viewed in the online issue, which is available at wileyonlinelibrary.com.]

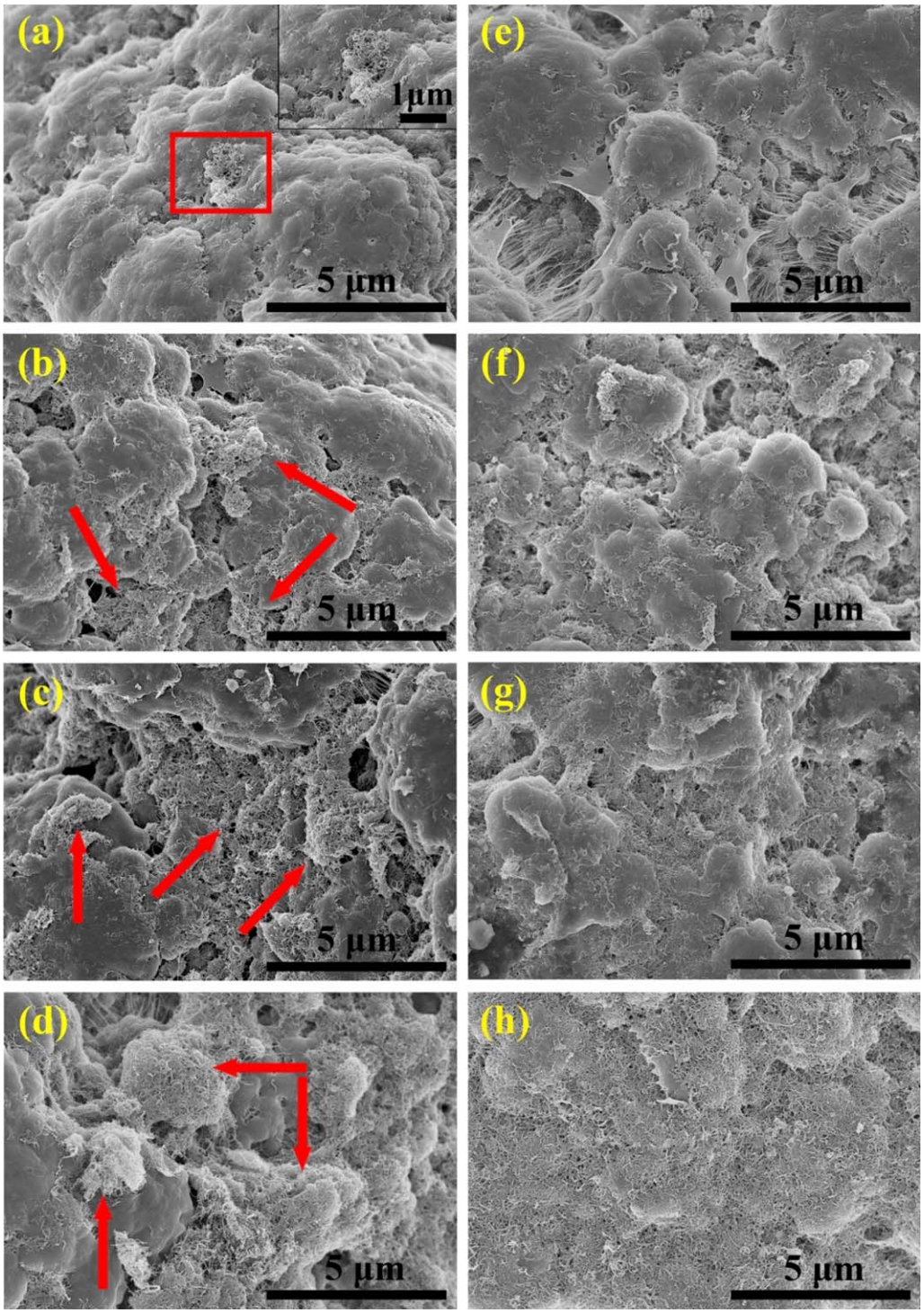

Figure 3. SEM images of UHMWPE/CNTs powders prepared by different methods of heat-drying (a–d) and freeze-drying (e–h). CNT content: (a, e) 0.05 wt %, (b, f) 0.5 wt %, (c, g) 1 wt %, (d, h) 2 wt %. [Color figure can be viewed in the online issue, which is available at wileyonlinelibrary.com.]

particles connected by nanometer fibrils.[20] The surface of these particles is smooth, whereas the fibrils are straight and parallel to each other. As shown in Figure 2(b), CNTs used in this work are squiggly and different from the fibrils in UHMWPE powders. In addition, the inset of Figure 2(b) shows a typical TEM image of multi-wall CNTs with inside hollow structure.

In order to illustrate the distribution state of CNTs at the surface of UHMWPE powders prepared by different drying methods, the SEM images of the prepared samples are displayed in Figure 3. Morphologies of the UHMWPE/CNTs powders prepared by heat drying are presented in Figure 3(a–d). Even at low CNT content of 0.05 wt %, there are some large CNT

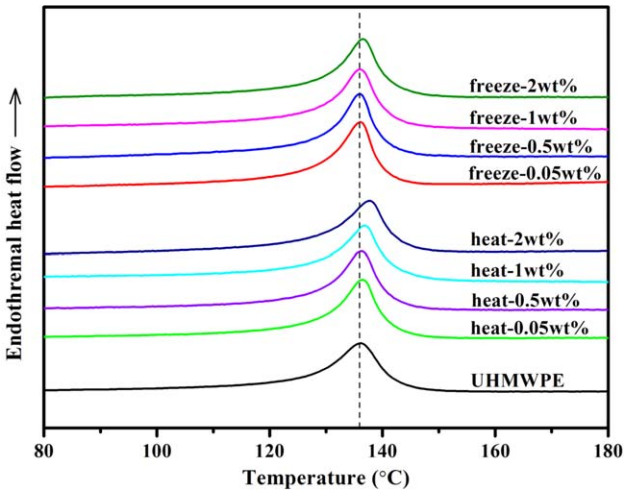

Figure 4. DSC curves for pure UHMWPE sample and UHMWPE/CNTs composites fabricated by different methods of heat-drying and freeze-drying. [Color figure can be viewed in the online issue, which is available at wileyonlinelibrary.com.]

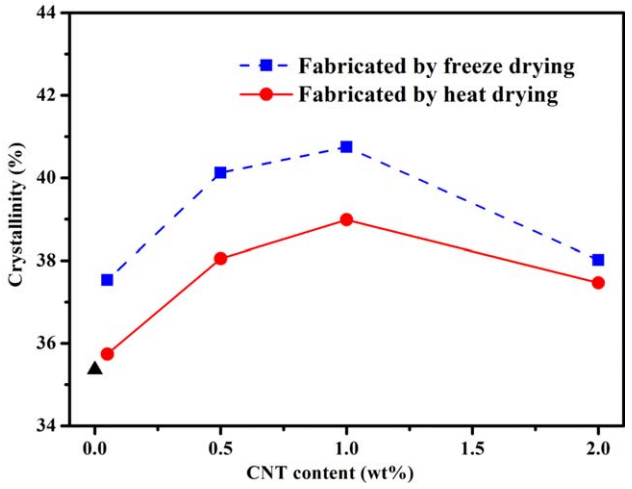

Figure 6. Effect of drying methods on crystallinity of UHMWPE/CNTs composites. [Color figure can be viewed in the online issue, which is available at wileyonlinelibrary.com.]

agglomerates [Figure 3(a and the inset of it]. With increasing content of CNTs, more CNTs appear at the surface of UHMWPE powders, and CNT agglomeration becomes more serious [Figure 3(a–d)]. When CNT content reaches 2 wt %, these CNT agglomerations even turn into microspheres [Figure 3(d)]. Similar phenomenon has been reported in some other researches.[21,22]

Figure 3(e–h) show the morphologies of the UHMWPE/CNTs powders fabricated by freeze-drying method. They are quite different from that in Figure 3(a–d). At 0.05 wt % CNT content, CNTs almost separate from each other and uniformly distribute at the surface of UHMWPE powders [Figure 3(e)]. When CNT content increases from 0.05 to 2 wt %, the surface of UHMWPE powders are gradually strewn by CNTs [Figure 3(e–h)]. With the content of 2 wt %, CNTs almost fully cover the surface of UHMWPE powders [Figure 3(h)].

In brief, the results indicate that freeze-drying method could produce CNTs-coated UHMWPE powders with optimized micromorphologies. It can be explained as follows. Using the heat-drying method, the dispersion medium of liquid water is gradually evaporated and slowly reduces the distance among CNTs. The mobile CNTs in fluid medium make it easier to agglomerate resulting from the existence of Van der Waals forces.[23] In contrast, the liquid water is previously frozen by liquid nitrogen, and then sublimate directly in the process of freeze-drying, by passing the fluid state. So when freeze-drying method is applied, the movement of CNTs is limited, thus the phenomenon of agglomeration is effectively prevented. Such effect of different drying methods on CNT distribution status is shown in a schematic diagram (Figure 1).

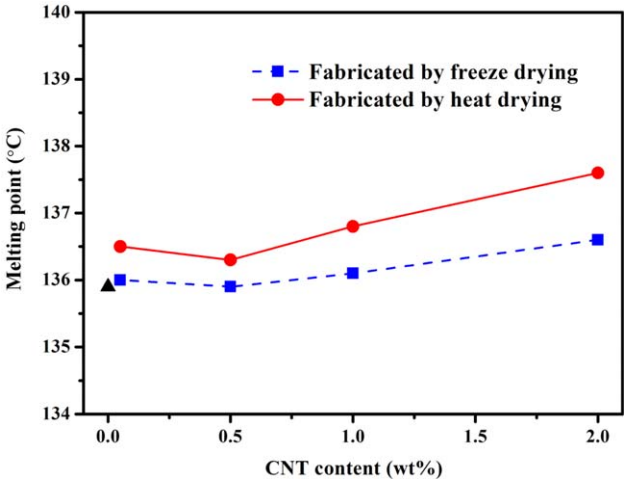

Figure 5. Effect of drying methods on melting point of UHMWPE/CNTs composites. The black point represents the melting point of UHMWPE. [Color figure can be viewed in the online issue, which is available at wileyonlinelibrary.com.]

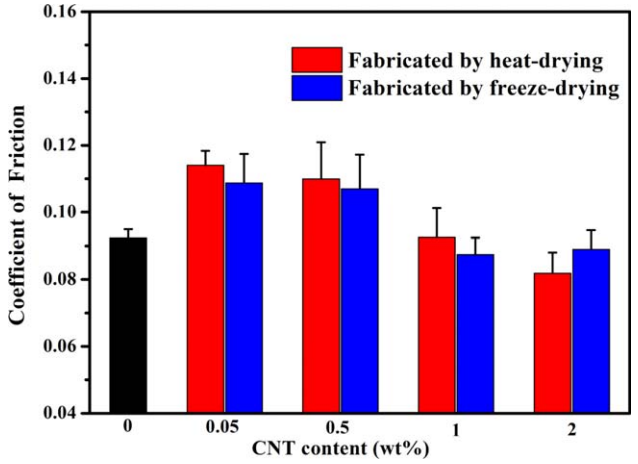

Figure 7. Coefficient of friction of UHMWPE/CNTs composites. [Color figure can be viewed in the online issue, which is available at wileyonlinelibrary.com.]

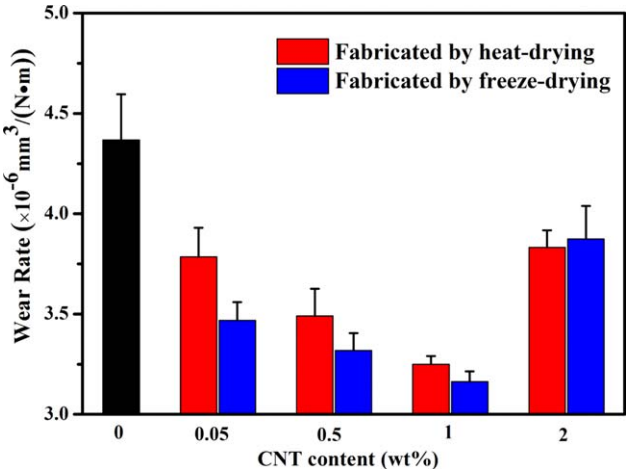

Figure 8. Wear rate of UHMWPE/CNTs composites. [Color figure can be viewed in the online issue, which is available at wileyonlinelibrary.com.]

Effect of CNT Distribution on the Crystallization of UHMWPE/CNTs Composites

To further explicate the influence of the drying methods on the crystallization behavior of UHMWPE/CNT composites, DSC tests were conducted. The heating thermograms are shown in Figure 4. On the basis of peak temperature of UHMWPE, the thermograms of composites prepared by heat-drying method (h-UHMWPE/CNTs) significantly shift to the right at high CNT content, but the shift is much smaller as for the composites prepared by freeze-drying method (f-UHMWPE/CNTs).

The peak temperature of the melting thermogram is defined as the melting point (T_m). Figure 5 shows the variations of T_m. The T_m value of pure UHMWPE is about 136°C. With the increasing content of CNTs, T_m exhibits an increased trend. Besides, T_m of h-UHMWPE/CNTs is always higher than that of f-UHMWPE/CNTs at the same loading of CNTs. This is particularly apparent in composites at higher CNT content.

In general, the melting point has a close link to the crystal size.[24,25] Under the assumption of a rectangular shaped crystal, the relationship is described using Thomson–Gibbs equation:[26]

$$T_m = T_m^0\left[1-\left(\frac{\sigma_1}{L_1}+\frac{\sigma_2}{L_2}+\frac{\sigma_3}{L_3}\right)\frac{2}{\rho_C \Delta H_m^0}\right] \quad (1)$$

Where $T_m^0 = 419$ K is the equilibrium melting temperature of the crystal with infinite thickness. σ_1, σ_2, and σ_3, with value of 94, 13.8, and 13.8 mJ/m^2, respectively, are the surface free energy. L_1, L_2, and L_3 are the dimensions of the crystallite. The $\rho_c = 1.0$ g/cm^3 is the crystal density, and $\Delta H_m^0 = 293$ J/g is the heat of fusion per unit mass of equilibrium melting.[27] The eq. (1) indicates that the melting point is directly proportional to the dimension of crystallite (L_1, L_2, L_3). Hence, according to the variation tendency of T_m (Figure 5), the average size of PE crystals should be increased with the addition CNT content, and the size in h-UHMWPE/CNTs would be larger than that in f-UHMWPE/CNTs.

Furthermore, based on the DSC curves, the heat of fusion (ΔH_m), and crystallinity (X_C) of the UHMWPE/CNTs composites were determined. The crystallinity was calculated from the endothermic peak using the formula below:

$$X_C = \frac{\Delta H_m}{\Delta H_m^0}\times 100\% \quad (2)$$

Where $\Delta H_m^0 = 293$ J/g is the heat of fusion for 100% of crystalline UHMWPE.[28] As calculated by the eq. (2), the crystallinity is shown in Figure 6. For the CNT modified composites, X_C increases with the increasing content of CNTs followed by a decrease when CNT content is over 1 wt %. High specific surface can make CNTs be regarded as nucleation sites, which might facilitate the nucleation and increased crystallinity.[29] However, excessive CNTs restrict the motion of molecular chains, resulting in the decreased X_C value.[30]

Besides, X_C value of f-UHMWPE/CNTs composite is always higher than that of h-UHMWPE/CNTs at the same content of CNTs, as shown in Figure 6. At the CNT content of 0.05 wt %, X_C of h-UHMWPE/CNTs is very close to that of UHMWPE samples, whereas is 6.15% lower than that of f-UHMWPE/CNTs. Basically, the improvement of X_C depends on the increase of average size or/and quantity of crystals. As discussed earlier, the average size of crystal in f-UHMWPE/CNTs should be smaller than that in h-UHMWPE/CNTs. Consequently, the amount of crystals would be much larger in f-UHMWPE/CNTs. It is possible to infer that, by utilizing the freeze-drying method, the CNTs distribute uniformly in the UHMWPE/CNTs composites, and provide much more nucleation sites. Therefore, the

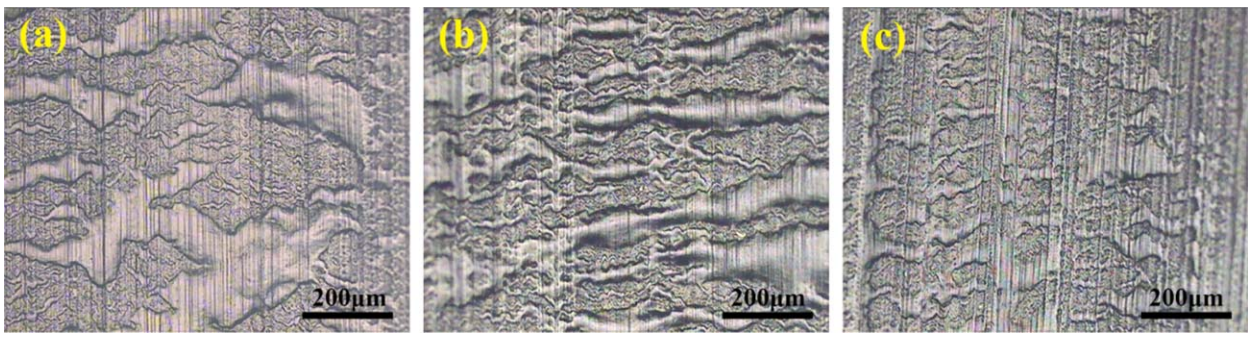

Figure 9. Optical images of worn surface: (a) pure UHMWPE, (b) and (c) are UHMWPE/CNTs composites with CNT content of 1 wt % prepared by heat-drying and freeze-drying, respectively. [Color figure can be viewed in the online issue, which is available at wileyonlinelibrary.com.]

quantity of crystals and the degree of crystallinity are improved conspicuously.

Tribological Properties of the UHMWPE/CNTs Composites

Wear tests were conducted to evaluate the tribological performance of the UHMWPE/CNTs composites. The variations in the coefficient of friction (COF) of the composites are demonstrated in Figure 7. At CNT content of 0.05 wt %, the COF is obviously increased by more than 20%. While at higher CNT content, the COF is observed to decrease. This can be due to the good mechanical properties and layered graphite structure of CNTs. At low CNT content, the shear strength of the composite should be improved significantly.[31] Increasing CNT content in composites inevitably leads to higher CNT fraction on the sample surface. Gradually, the self-lubricating effects would become a key factor in friction process, which contributes to the reduction in the coefficient of friction.

However, compared with the variation of the COF, Figure 8 shows the opposite trend: the wear rate decreases dramatically at first, whereas it increases at the high content of 2 wt %. When CNT content reaches 1 wt %, the composites possess the best tribological performance, and the wear rate of h-UHMWPE/CNTs and f-UHMWPE/CNTs composite decreases by 25.6% and 27.6%, respectively, compared with that of the pure UHMWPE material. Moreover, the results show a distinct phenomenon that the wear resistance of f-UHMWPE/CNTs significantly outperforms that of h-UHMWPE/CNTs, when CNT content does not exceed 1 wt %. For instance, at CNT content of 0.05 wt %, the wear rate of h-UHMWPE/CNTs is 9.15%, higher than that of f-UHMWPE/CNTs.

The worn surfaces of typical samples are shown in Figure 9. For pure UHMWPE, the worn surface has deep grooves and serous fatigue-separated layers, which correspond to the wear mechanisms of abrasive and fatigue wear, respectively.[32] From Figure 9(a–c), the size of fatigue-separated layers gradually decrease. This indicates that the fatigue wear can effectively weaken by incorporation of CNTs, and such effect would be more significant for the UHMWPE/CNTs composites fabricated by freeze-drying method.

Wear properties of UHMWPE/CNTs composites are partly determined by the CNT distribution status. As discussed in the previous section, freeze-drying method has an obvious advantage in ameliorating the dispersion state of CNTs in the composites, compared to the heat-drying method. Thus, during wear tests, the stress would be more effectively transferred by the filler of CNTs in the f-UHMWPE/CNTs composites, which results in lower fatigue wear and wear rate.

Furthermore, the crystallinity also plays an important role in the tribological performance of UHMWPE/CNTs composites. As a semicrystalline polymer, the crystalline phase alignment under pressure during wear process.[33] An energy-based model suggests the wear rate of UHMWPE should be only dependent on energy dissipation.[34] Hence, improving crystallinity of UHMWPE should facilitate dissipate energy and decrease wear rate, given that scratch on crystals requires higher energy. It has also been demonstrated in the experiment that a higher degree of crystallinity in the UHMWPE for slowly cooling rate would lead to an increase in scratch resistance and lower COF.[35] From this point, it can be concluded that improved crystallinity of UHMWPE for the presence of CNTs can enhance wear resistance of UHMWPE based composites.

Through above analysis, it is easy to understand that why freeze-drying method has a positive impact on the wear properties of UHMWPE/CNTs composites. Because of the optimized CNT dispersion and higher crystallinity, the stress can be transferred more effectively, and more energy is dissipated during wear tests, leading to the dramatically decreased wear rates of f-UHMWPE/CNTs composites at low CNT content.

CONCLUSIONS

In this study, UHMWPE/CNTs composites with optimized micromorphologies were fabricated by freeze-drying method. CNTs uniformly dispersed at the surface of UHMWPE powders and in the UHMWPE/CNTs composites. They provided more nucleation sites during hot-press process, and improved the quantity of crystals and the degree of crystallinity in composites. Better CNT distribution and higher crystallinity resulted in the enhanced tribological performances of UHMWPE/CNTs materials. In addition, the freeze-drying method is low cost and environment friendly, which can be applied to industrial production.

ACKNOWLEDGMENTS

The authors gratefully acknowledge the support from the Ministry of Science and Technology of China (Grant No. 2011CB606405), the National Nature Science Foundation of China (Grant No. 51232005), Shenzhen Projects for Basic Research (Grant Nos. JC201105201119A and JCYJ20120831165730910), Guangdong Province Innovation R&D Team Plan for Energy and Environmental Materials (Grant No.2009010025), and the Kone China Co. Ltd.

REFERENCES

1. Samad, M. A.; Sinha, S. K. *Wear* **2011**, *270*, 395.
2. Kurtz, S. M. UHMWPE Biomaterials Handbook; Academic Press: Waltham, **2009**; p 1.
3. Samad, M. A.; Sinha, S. K. *Tribol. Int.* **2011**, *44*, 1932.
4. Chang, B. P.; Akil, H. M.; Nasir, R. B. M. *Wear* **2013**, *297*, 1120.
5. Huang, A.; Su, R.; Liu, Yanqing *J. Appl. Polym. Sci.* **2013**, *129*, 1218.
6. Ge, S.; Wang, S.; Huang, X. *Wear* **2009**, *267*, 770.
7. Chang, B. P.; Akil, H. M.; Nasir, R. B. M.; Bandara, I. M. C. C. D.; Rajapakse, S. J. *Reinf. Plast. Compos.* **2014**, *33*, 674.
8. Al-Saleh, M. H.; Jawad, S. A.; Ghanem, H. M. E. *High Perform. Polym.* **2014**, *26*, 205.
9. Kanagaraj, S.; Mathew, M. T.; Fonseca, A.; Oliveira, M. S. A.; Simoes, J. A. O.; Rocha, L. A. *Int. J. Surf. Sci. Eng.* **2010**, *4*, 305.

10. Zoo, Y. S.; An, J. W.; Lim, D. P.; Lim, D. S. *Tribol. Lett.* **2004**, *16*, 305.
11. Xi, Y.; Yamanaka, A.; Bin, Y.; Matsuo, M. *J. Appl. Polym. Sci.* **2007**, *105*, 2868.
12. Sánchez, Y.; Albano, C.; Karam, A.; Perera, R.; Casas, E. *Macromol. Symp.* **2009**, *282*, 185.
13. Park, H. J.; Kim, J.; Seo, Y.; Shim, J.; Sung, M. Y.; Kwak, S. *Macromol. Res.* **2013**, *21*, 965.
14. Wanga, B.; Lia, H.; Lia, L.; Chena, P.; Wang, Z. *Compos. Sci. Technol.* **2013**, *89*, 180.
15. Dong, L.; Li, Y.; Wang, L.; Wan, Z.; Hou, F.; Liu, J. *J. Mater. Sci.* **2014**, *49*, 4979.
16. Dong, L.; Hou, F.; Li, Y.; Wang, L.; Gao, H.; Tang, Y. *Compos. Part A-Appl. Sci. Manuf.* **2014**, *56*, 248.
17. Ratti, C. J. *Food Eng.* **2001**, *49*, 311.
18. Abascal, K.; Ganora, L.; Yarnell, E. *Phytother. Res.* **2005**, *19*, 655.
19. Dong, L.; Li, Y.; Wang, L.; Xu, S.; Hou, F. *Mater. Lett.* **2014**, *130*, 180.
20. Clark, A. C.; Ho, S. P.; LaBerge, M. *Tribol. Int.* **2006**, *39*, 1327.
21. Liu, Y.; Sinha, S. K. *Wear.* **2013**, *300*, 44.
22. Pang, H.; Xu, L.; Yan, D. X.; Li, Z. M. *Prog. Polym. Sci.* **2014**, *39*, 1908.
23. Ma, P. C.; Mo, S. Y.; Tang, B. Z.; Kim, J. K. *Carbon* **2010**, *48*, 1824.
24. Xue, Y.; Zhao, Q.; Luan, C. *J. Colloid Interf. Sci.* **2001**, *243*, 388.
25. Jiang, Q.; Yang, C. C.; Li, J. C. *Macromol. Theory Simul.* **2003**, *12*, 57.
26. Gedde, U. W. Polymer Physics; Chapman and Hall: London, **1995**; p 144.
27. Shin, K.; Woo, E.; Jeong, Y. G.; Kim, C.; Huh, J.; Kim, K. W. *Macromolecules* **2007**, *40*, 6617.
28. Wunderlich, B. Macromolecular Physics; Academic Press: New York, **1973**; Vol. *3*, p 39.
29. Xua, G.; Zhuang, Y.; Xia, R.; Cheng, J.; Zhang, Y. *Mater. Lett.* **2012**, *89*, 272.
30. Xu, J. Z.; Zhong, G. J.; Hsiao, B. S.; Fu, Q.; Li, Z. M. *Prog. Polym. Sci.* **2014**, *39*, 555.
31. Samad, M. A.; Sinha, S. K. *Tribol. Int.* **2011**, *44*, 1932.
32. An, Y.; Tai, Z.; Qi, Y.; Yan, X.; Liu, B.; Xue, Q.; Pei, J. *J. Appl. Polym. Sci.* **2014**, 39640.
33. Galetz, M. C.; Glatzel, U. *Tribol. Lett.* **2010**, *38*, 1.
34. Colaço, R.; Gispert, M. P.; Serro, A. P.; Saramago, B. *Tribol. Lett.* **2007**, *26*, 119.
35. Karuppiah, K. S. K.; Bruck, A. L.; Sundararajan, S.; Wang, J.; Lin, Z.; Xu, Z. H.; Li, X. *Acta Biomater.* **2008**, *4*, 1401.